

Volume Dependence of the Pion Mass from Renormalization Group Flows

B. Klein^{1*},[†], J. Braun[†] and H.J. Pirner^{†, **}

^{*}*GSI, Planckstrasse 1, 64291 Darmstadt, Germany*

[†]*Institute for Theoretical Physics, University of Heidelberg, Philosophenweg 19, 69120 Heidelberg, Germany*

^{**}*Max-Planck-Institut für Kernphysik, Saupfercheckweg 1, 69117 Heidelberg, Germany*

Abstract. We investigate finite volume effects on the pion mass and the pion decay constant with renormalization group (RG) methods in the framework of a phenomenological model for QCD. An understanding of such effects is important in order to interpret results from lattice QCD and extrapolate reliably from finite lattice volumes to infinite volume.

We consider the quark-meson-model in a finite Euclidean $3+1$ dimensional volume. In order to break chiral symmetry in the finite volume, we introduce a small current quark mass. In the corresponding effective potential for the meson fields, the chiral $O(4)$ -symmetry is broken explicitly, and the sigma and pion fields are treated individually. Using the proper-time renormalization group, we derive renormalization group flow equations in the finite volume and solve these equations in the approximation of a constant expectation value.

We calculate the volume dependence of pion mass and pion decay constant and compare our results with recent results from chiral perturbation theory in finite volume.

Keywords: Renormalization group, chiral perturbation theory, finite volume effects, lattice gauge theory

PACS: 12.38.Lg, 12.39.Fe

1. INTRODUCTION

Two important motivations inspire us to study QCD in a finite volume: a generic interest in finite volume effects, and the separation of scales afforded by the additional length scale. Among nonperturbative methods used in the study of QCD, lattice simulations have a very important place. However, they are necessarily performed in relatively small volumes, and a good understanding of finite volume effects is required for an extrapolation to infinite volume. Typically, lattice sizes are of the order of $L \lesssim 2 - 3$ fm, while pion masses are of the order $m_\pi \gtrsim 500 - 700$ MeV [1, 2]. Thus, we require tools to describe the volume dependence of observables in these regimes. In this work, our objective is to describe the volume dependence of two of the low energy observables, the pion mass and the pion decay constant, and to provide a model for finite volume effects across a wide range of length scales.

The low energy behavior of QCD is determined by spontaneous chiral symmetry breaking [3]: As a consequence, massless Goldstone bosons associated with the broken symmetries emerge, and the low energy limit can be described by an effective

¹ email: b.klein@gsi.de

theory of these light, weakly interacting degrees of freedom. Such descriptions in terms of light degrees of freedom only become even better in finite Euclidean volumes: contributions of heavier particles are suppressed by e^{-ML} , where M is the typical separation of the hadronic mass scale from the Goldstone masses. Therefore, a second motivation to study finite volume QCD is that it allows isolation of the low-energy behavior and a description in terms of the Goldstone modes.

Different approaches based on this idea have proven very fruitful: Chiral perturbation theory makes predictions for the volume and temperature dependence of pion mass, pion decay constant and chiral condensate [4, 5, 6], finite volume partition functions [7] and random matrix theory [8, 9] predict eigenvalue spectra, and the dependence of the chiral condensate on volume and quark mass [10].

The most important results in the present context are those from chiral perturbation theory (chPT), which relies on an expansion in terms of the three-momentum $|\vec{p}|$ and the pion mass m_π , which are small compared to the chiral symmetry breaking scale $4\pi f_\pi$. Consequently, a finite volume places constraints on the expansion, since the smallest momentum is determined by the volume, $p_{\min} \sim \frac{2\pi}{L}$, and requires different expansion schemes, depending on the relative size of L and $1/m_\pi$.

A very useful result obtained by Lüscher [11] relates the leading corrections to the pion mass in finite Euclidean volume to the $\pi\pi$ -scattering amplitude in infinite volume. The relative shift $R[m_\pi(L)]$ of the pion mass $m_\pi(L)$ in finite volume compared to its value $m_\pi(\infty)$ in infinite volume is according to this result given by

$$\begin{aligned} R[m_\pi(L)] &= \frac{m_\pi(L) - m_\pi(\infty)}{m_\pi(\infty)} \\ &= -\frac{3}{16\pi^2} \frac{1}{m_\pi} \frac{1}{m_\pi L} \int_{-\infty}^{\infty} dy F(iy) e^{-\sqrt{m_\pi^2 + y^2} L} + \mathcal{O}(e^{-\bar{m}L}). \end{aligned} \quad (1)$$

$F(s)$ is the forward $\pi\pi$ -scattering amplitude as a function of the energy variable s , continued to complex values, and the sub-leading corrections drop at least as $\mathcal{O}(e^{-\bar{m}L})$ where $\bar{m} \geq \sqrt{3/2}m_\pi$. New results have been obtained by using a calculation of the $\pi\pi$ -scattering amplitude in chPT to three loops (*nnlo*) as input for Lüscher's formula [12, 13]. The shift above the leading one-loop result from this approach can then be used to supplement the full one-loop calculation [5] for the mass shift in chPT.

However, this explanation relies purely on the “squeezing” of a “pion cloud” [1], whereas - albeit smaller - shifts of meson and hadron masses also appear in quenched lattice calculations, show a power law behavior for small L rather than the behavior expected from chPT [14, 15], and are generally underestimated [2]. This suggests that in addition to the pion effects, quark effects at higher momentum scales also contribute directly to the finite volume mass shifts.

In the present investigation, we thus use a phenomenological low-energy model which is suited to a description of dynamical chiral symmetry breaking and which incorporates heavy constituent quarks. As a drawback, this model is not a gauge theory and the constituent quarks are not confined, but decouple from the dynamics at low momenta only because of their large masses. Since spontaneous symmetry

breaking does not occur in a finite volume, the inclusion of a small quark mass, which explicitly breaks the chiral symmetry, is essential.

We employ an RG method in order to cover the relevant range of length scales and pion masses. Thus, we do not have to rely on either the box size or the pion mass as an expansion parameter: the RG flow equations remain valid as long as the model used as input does. The great advantage is precisely that the RG flow equations describe the connection between different momentum scales, and in the present case also the dependence on the additional scale $1/L$ introduced by the finite volume.

2. RENORMALIZATION GROUP FLOW EQUATIONS

In the present work, we use the two-flavor quark-meson model, an $O(4)$ -invariant linear sigma model where the meson fields $\phi = (\sigma, \vec{\pi})$ are coupled to two constituent quarks through an $SU(2) \otimes SU(2)$ -invariant interaction term. It is an effective model for dynamical chiral symmetry breaking below a scale $\Lambda \simeq 1.5$ GeV, where a description of QCD in terms of hadronic degrees of freedom is valid. Although the linear sigma-model by itself is not compatible with the low-energy $\pi\pi$ -scattering data, due to the presence of quarks the low energy constants of chiral perturbation theory are reproduced [16].

We consider the model in a four-dimensional Euclidean volume with compact Euclidean space and time directions. The bare effective action at the scale Λ is

$$\Gamma_\Lambda[\phi] = \int d^4x \left\{ \bar{q}\gamma \cdot \partial q + g\bar{q}(m_c + \sigma + i\vec{\tau} \cdot \vec{\pi}\gamma_5)q + \frac{1}{2}(\partial_\mu\phi)^2 + U_\Lambda(\phi) \right\}, \quad (2)$$

where the quark mass term gm_c explicitly breaks the chiral symmetry. At the scale Λ , the meson potential can be characterized by the values of two couplings:

$$U_\Lambda(\phi) = \frac{1}{2}m_{UV}^2\phi^2 + \frac{1}{4}\lambda_{UV}(\phi^2)^2. \quad (3)$$

In Gaussian approximation, the one-loop effective action for the scalar fields is

$$\Gamma[\phi] = \Gamma_\Lambda[\phi] - \text{Tr} \log \left(\Gamma_F^{(2)}[\phi] \right) + \frac{1}{2} \text{Tr} \log \left(\Gamma_B^{(2)}[\phi] \right), \quad (4)$$

where $\Gamma_B^{(2)}[\phi]$ and $\Gamma_F^{(2)}[\phi]$ are the inverse two-point functions for the bosonic and the fermionic fields, evaluated at the expectation value of the mesonic field, ϕ . We consider an approximation where the field ϕ is constant over the entire volume and the effective action is reduced to an effective potential, $\Gamma[\phi] = \int d^4x U(\phi)$. To regularize the functional traces, we use a Schwinger proper-time representation of the logarithms. The dependence on a cutoff scale k is introduced through an infrared cutoff function $f_a(\tau k^2)$ of the form

$$k \frac{\partial}{\partial k} f_a(\tau k^2) = -\frac{2}{a!}(\tau k^2)^{a+1} \exp(-\tau k^2) \quad (5)$$

which satisfies all required regularization conditions [17, 18]. For reasons of convergence of the momentum integrals, we use $a = 2$. Such a cutoff function makes it possible to systematically integrate out only those quantum fluctuations around the expectation value which have momenta above the scale k .

We now wish to obtain a renormalization group flow equation for the effective action, which describes how the couplings in the action change with a change of the renormalization scale k . We arrive at such an equation by taking the derivative of the regularized expression for the effective action with respect to this scale k , and then replacing the bare two-point function from the original expression by the renormalized two-point functions, which contain the scale-dependent couplings:

$$\begin{aligned} k \frac{\partial}{\partial k} \Gamma_k[\phi] &= \frac{1}{2} \text{Tr} \int_0^\infty \frac{d\tau}{\tau} \left[k \frac{\partial}{\partial k} f_a(\tau k^2) \right] \exp[-\tau \Gamma_{B,k}^{(2)}[\phi]] \\ &\quad - \text{Tr} \int_0^\infty \frac{d\tau}{\tau} \left[k \frac{\partial}{\partial k} f_a(\tau k^2) \right] \exp[-\tau \Gamma_{F,k}^{(2)}[\phi]]. \end{aligned} \quad (6)$$

Note that boundary conditions for the fields are implicit in the traces. In Euclidean time direction, the sum over bosonic and fermionic Matsubara frequencies can be done analytically [19] before the zero temperature limit is taken. In infinite volume, the momentum integrations for the spatial directions can be performed as well, and the flow equation becomes

$$k \frac{\partial}{\partial k} U_k(\sigma, \vec{\pi}^2, L \rightarrow \infty) = \frac{k^6}{32\pi^2} \left(-\frac{4N_c N_f}{k^2 + M_q^2} + \sum_{i=1}^4 \frac{1}{k^2 + M_i^2} \right). \quad (7)$$

In finite volume, the momentum integrations become sums over momentum modes. Choosing anti-periodic boundary conditions for the fermionic fields also in the spatial directions, we define

$$p_F^2 = \sum_{i=1}^{d-1} p_i^2 = \frac{4\pi^2}{L^2} \sum_{i=1}^{d-1} \left(n_i + \frac{1}{2} \right)^2, \quad p_B^2 = \sum_{i=1}^{d-1} p_i^2 = \frac{4\pi^2}{L^2} \sum_{i=1}^{d-1} n_i^2. \quad (8)$$

The RG flow equation for the meson potential in finite volume then reads

$$k \frac{\partial}{\partial k} U_k(\sigma, \vec{\pi}^2, L) = \frac{3}{16} \frac{k^6}{L^3} \sum_{\vec{n}} \left(-\frac{4N_c N_f}{(k^2 + p_F^2 + M_q^2)^{5/2}} + \sum_{i=1}^4 \frac{1}{(k^2 + p_B^2 + M_i^2)^{5/2}} \right). \quad (9)$$

The meson masses $M_i^2(\sigma, \vec{\pi}^2)$ are the eigenvalues of $[U_k''(\sigma, \vec{\pi}^2)]^{ij}$, the second derivative matrix of the meson potential. In the presence of a finite current quark mass gm_c , the quark mass $M_q^2(\sigma, \vec{\pi}^2) = g^2[(\sigma_0 + m_c)^2 + 2m_c(\sigma - \sigma_0) + (\sigma^2 + \vec{\pi}^2 - \sigma_0^2)]$ contains explicitly symmetry breaking terms. Since symmetry breaking terms appear only here and are all of this form, we make for the meson potential the ansatz

$$U_k(\sigma, \vec{\pi}^2) = \sum_{i=0}^4 \sum_{j=0}^{[\frac{1}{2}(4-i)]} a_{ij}(k) (\sigma - \sigma_0(k))^i (\sigma^2 + \vec{\pi}^2 - \sigma_0(k)^2)^j. \quad (10)$$

It depends only on $\vec{\pi}^2$ since the symmetry of the pion subspace remains unbroken.

TABLE 1. Values for the parameters at the *UV*-scale Λ which were used in the numerical evaluation. The parameters are obtained by fitting the results of the RG evolution to a particular pion mass and the corresponding pion decay constant in infinite volume. The physical current quark mass corresponds to gm_c .

Λ [MeV]	m_{UV} [MeV]	λ_{UV}	gm_c [MeV]	f_π [MeV]	m_π [MeV]
1500	779.0	60	2.10	90.38	100.8
1500	747.7	60	9.85	96.91	200.1
1500	698.0	60	25.70	105.30	300.2

3. RESULTS OF THE NUMERICAL CALCULATIONS

We solve the RG flow equations numerically for infinite and finite volume. In order to do this, we insert the ansatz (10) into the flow equations (7),(9) and obtain a set of coupled, ordinary differential equations for the couplings $a_{ij}(k)$ and the minimum $\sigma_0(k)$. We choose initial values for the couplings at the scale $k = \Lambda$ and evolve the couplings until at $k \rightarrow 0$ all quantum fluctuations have been integrated out. Pion mass and pion decay constant are extracted from the resulting effective potential. For the case of finite volume, the sums over the momentum modes need to be truncated at a finite number of modes. For the results presented here, where we use $n_{\max} = 40$, the effects of this truncation are negligible [20].

In TAB. 1, we give an overview over the three parameter sets we have used to obtain results for pion masses of 100, 200 and 300 MeV. These parameters are obtained by fitting so that the results of the RG evolution match a particular value of the pion mass $m_\pi(\infty)$ and the corresponding value of the pion decay constant $f_\pi(\infty)$ from chPT in infinite volume. With these fixed parameter values, we solve the finite volume RG equations, which gives a prediction for the volume dependence of $m_\pi(L)$ and $f_\pi(L)$. The coupling g does not evolve in our approximation and was set to $g = 3.26$, which leads to a reasonable constituent quark mass for physical values of f_π and m_π . We present our results for the volume dependence of the pion mass in FIGS. 1-3 and numerical values for select volumes in TAB. 2. We will focus on these results for the pion mass, since they are more easily accessible on the lattice than the pion decay constant. For the results on $f_\pi(L)$, we refer to [20].

FIGS. 1-3 show the relative change $R[m_\pi(L)] = \frac{m_\pi(L) - m_\pi(\infty)}{m_\pi(\infty)}$ of the pion mass in finite volume $m_\pi(L)$ compared to the value $m_\pi(\infty)$ in infinite volume as a function of the volume size L . We plot the results for the pion masses $m_\pi(\infty) = 100, 200, 300$ MeV on a logarithmic scale. For comparison, we plot in addition the one-loop chPT result of [5], and the one-loop chPT result with corrections to three-loop order obtained with the Lüscher formula [12].

The relative change of the pion mass decreases with increasing volume size. The RG results are consistently above the results from chPT. Higher loop order corrections in chPT increase the mass shift predicted by chPT, and the difference

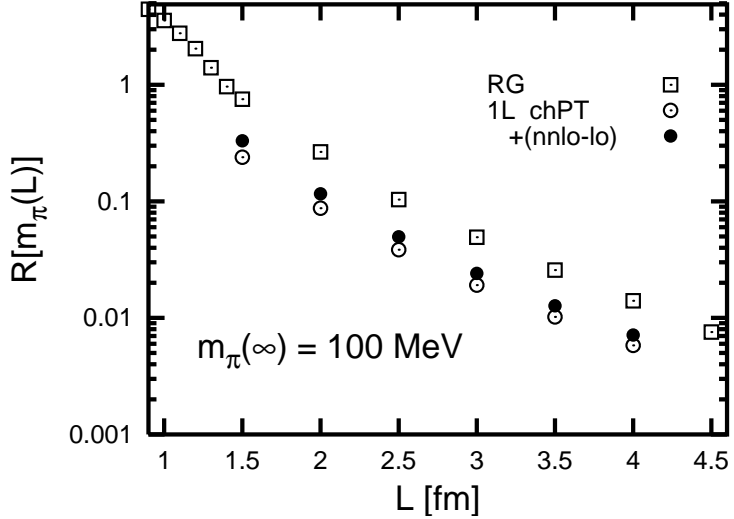


FIGURE 1. Volume dependence of the pion mass for a value $m_\pi(\infty) = 100$ MeV in infinite volume. We plot the relative shift of the pion mass from its infinite volume limit $R[m_\pi(L)] = (m_\pi(L) - m_\pi(\infty))/m_\pi(\infty)$ as a function of the size of the volume L . For comparison to the RG result, we also plot the results from chPT calculations taken from [12] for the full one-loop result (1L chPT) and with $nnlo$ -corrections (1L chPT + ($nnlo-lo$)).

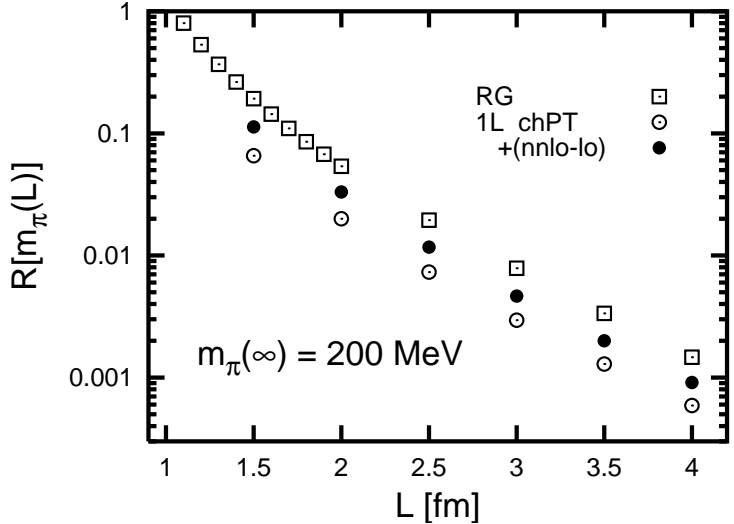


FIGURE 2. Volume dependence of the pion mass for a value $m_\pi(\infty) = 200$ MeV in infinite volume. For a detailed explanation, see caption of FIG. 1. Note the different scales on the axes for different values of $m_\pi(\infty)$.

to the RG result becomes smaller. We note that the relative size of the higher loop order corrections to the one-loop chPT result become larger with larger pion mass. This is not unexpected, since Lüscher's formula becomes an increasingly better approximation with increasing pion mass for a given volume size. For larger volumes, the differences between the RG result and the one-loop chPT

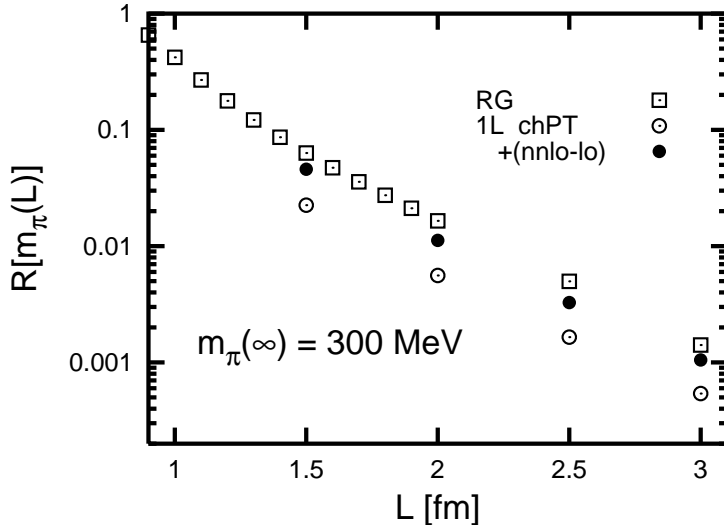


FIGURE 3. Volume dependence of the pion mass for a value $m_\pi(\infty) = 300$ MeV in infinite volume. For a detailed explanation, see caption of FIG. 1. Note the different scales on the axes for different values of $m_\pi(\infty)$.

TABLE 2. Values for $R[m_\pi(L)]$, the relative shift of the pion mass in finite volume compared to the value in infinite volume (cf. eq. (1)). We show results for volume sizes $L = 2.0, 2.5, 3.0$ fm, and for pion masses $m_\pi(\infty) = 100, 200, 300$ MeV. The RG results are compared to the exact one-loop chPT results of [5] (1L chPT), and to the exact one-loop calculation with corrections in three-loop order obtained with chPT and Lüscher's formula [12] (1L chPT + ($nnlo-lo$))). In the last column, the difference ΔR between the RG result and the three-loop corrected chPT result is given.

L [fm]	$m_\pi(\infty)$ [MeV]	$m_\pi L$	$R[m_\pi(L)]$			ΔR
			RG	1L chPT	+($nnlo-lo$)	
2.0	100	1.01293	26.6×10^{-2}	8.74×10^{-2}	11.6×10^{-2}	15.0×10^{-2}
	200	2.02586	5.38×10^{-2}	2.00×10^{-2}	3.31×10^{-2}	2.07×10^{-2}
	300	3.03879	1.70×10^{-2}	0.56×10^{-2}	1.12×10^{-2}	0.58×10^{-2}
2.5	100	1.26616	10.37×10^{-2}	3.85×10^{-2}	4.97×10^{-2}	5.40×10^{-2}
	200	2.53233	1.95×10^{-2}	0.73×10^{-2}	1.17×10^{-2}	0.78×10^{-2}
	300	3.79849	5.31×10^{-3}	1.65×10^{-3}	3.27×10^{-3}	2.04×10^{-3}
3.0	100	1.5194	4.94×10^{-2}	1.91×10^{-2}	2.41×10^{-2}	2.53×10^{-3}
	200	3.03879	7.85×10^{-3}	2.95×10^{-3}	4.65×10^{-3}	3.20×10^{-3}
	300	4.55819	1.76×10^{-3}	0.54×10^{-3}	1.05×10^{-3}	0.71×10^{-3}

calculation with the corrections obtained with Lüscher's formula drop exponentially as $\exp(-cm_\pi L)$ with $c > 0$, compatible with the error estimate from Lüscher's result. As expected, for large volume the slopes of the chPT results and the RG results in the logarithmic plot are the same, since the mass shift is then due entirely to pion effects and thus should drop as $\exp(-m_\pi L)$. In contrast to chPT, the RG calculation can also be extended to very small volumes, where the chiral expansion

is considered unreliable, and describe the transition into the regime where chiral symmetry is effectively restored.

In our model, two effects are responsible for the finite volume mass shift. Chiral symmetry is broken dynamically and light Goldstone modes appear when the quark fields form a condensate. The presence of the additional scale $1/L$ affects this condensation. In a finite volume, the lowest possible momentum mode of the fermions is $\sqrt{3}\pi/L$. For small volumes, this acts as an infrared cutoff, which effectively “freezes” the quark fields so that fewer modes can contribute to the condensate. The mesonic fields, on the other hand, are much less affected by the finite volume, since the scale $2\pi/L$ imposes only a minimum for the smallest non-zero momentum mode. Fluctuations due to these light mesonic modes lead to a further decrease of the condensate, which in turn leads to the observed increase in the masses of the light mesons. These pion effects dominate for larger volumes, which explains the convergence of the RG and chPT results for large L .

4. CONCLUSIONS

We have presented a study of finite volume effects on the pion mass and on the pion decay constant. We have applied renormalization group methods to a phenomenological model of low-energy QCD with mesons and constituent quarks as degrees of freedom. We solved the resulting RG flow equations in finite volume. We stress the importance of taking explicit symmetry breaking into account and of considering pions and the sigma as individual degrees of freedom.

We compared our results for the volume dependence of the pion mass to recent results obtained in chiral perturbation theory. While they are compatible for small pion masses and large volumes, we find from the RG generally a larger mass shift than the one predicted by chiral perturbation theory. We explain this for small volumes by the effect of the additional IR cutoff L on the quark condensation, while for larger volumes the fluctuations due to light pions are the dominating effect. This view is supported by the convergence between the RG and chPT results for large volumes. Thus, the RG approach in a model including quarks provides a mechanism to qualitatively understand the volume dependence. The RG results remain valid even to very small volumes, where the chiral expansion becomes unreliable.

An important point that still requires careful investigation is the influence of the choice of the boundary conditions for the fermionic fields in the spatial directions. As on the lattice, where anti-periodic boundary conditions for quarks lead to a larger finite volume shift than periodic boundary conditions [14], we observe a dependence of our results on this choice. This will be the topic of future work.

ACKNOWLEDGMENTS

We would like to thank the organizers for a very pleasurable and inspiring meeting, for the hospitality in Belgium and for a thoroughly enjoyable experience. J.B. would like to thank the GSI for financial support.

REFERENCES

1. A. Ali Khan *et al.* [QCDSF-UKQCD Collaboration], Nucl. Phys. B **689** (2004) 175.
2. S. Aoki *et al.* [JLQCD Collaboration], Phys. Rev. D **68** (2003) 054502.
3. J. Gasser and H. Leutwyler, Annals Phys. **158** (1984) 142.
4. J. Gasser and H. Leutwyler, Phys. Lett. B **184** (1987) 83.
5. J. Gasser and H. Leutwyler, Phys. Lett. B **188** (1987) 477.
6. J. Gasser and H. Leutwyler, Nucl. Phys. B **307** (1988) 763.
7. H. Leutwyler and A. Smilga, Phys. Rev. D **46** (1992) 5607.
8. E. V. Shuryak and J. J. M. Verbaarschot, Nucl. Phys. A **560**, 306 (1993).
9. J. J. M. Verbaarschot, Phys. Rev. Lett. **72**, 2531 (1994).
10. J. J. M. Verbaarschot, Phys. Lett. B **368**, 137 (1996).
11. M. Lüscher, Commun. Math. Phys. **104** (1986) 177.
12. G. Colangelo and S. Dürr, Eur. Phys. J. C **33** (2004) 543.
13. G. Colangelo and C. Haefeli, Phys. Lett. B **590** (2004) 258.
14. S. Aoki *et al.*, Phys. Rev. D **50** (1994) 486.
15. M. Fukugita, H. Mino, M. Okawa, G. Parisi and A. Ukawa, Phys. Lett. B **294** (1992) 380.
16. D. U. Jungnickel and C. Wetterich, Eur. Phys. J. C **2**, 557 (1998).
17. B. J. Schaefer and H. J. Pirner, Nucl. Phys. A **660** (1999) 439.
18. G. Papp, B. J. Schaefer, H. J. Pirner and J. Wambach, Phys. Rev. D **61**, 096002 (2000).
19. J. Braun, K. Schwenzer and H. J. Pirner, Phys. Rev. D **70** (2004) 085016.
20. J. Braun, B. Klein and H. J. Pirner, Phys. Rev. D **71** (2005) 014032.